

Open clusters housing classical Cepheids in *Gaia* DR3

C. J. Hao^{1,2}, Y. Xu^{1,2}, Z. Y. Wu^{3,4}, Z. H. Lin^{1,2}, S. B. Bian^{1,2}, Y. J. Li¹, D. J. Liu^{1,2}

¹ Purple Mountain Observatory, Chinese Academy of Sciences, Nanjing 210023, PR China e-mail: xuye@pmo.ac.cn

² School of Astronomy and Space Science, University of Science and Technology of China, Hefei 230026, PR China

³ National Astronomical Observatories, Chinese Academy of Sciences, 20A Datun Road, Chaoyang District, Beijing 100101, PR China

⁴ School of Astronomy and Space Science, University of Chinese Academy of Sciences, Beijing 101408, PR China

Received 22 July 2022 / Accepted 23 September 2022

ABSTRACT

The latest *Gaia* Data Release 3 provides an opportunity to expand the census of Galactic open clusters harboring classical Cepheid variables, thereby bolstering the cosmic distance scale. A comprehensive analysis yielded a total of 50 classical Cepheids associated with 45 open clusters, of which 39 open cluster–classical Cepheid pairs are considered probable, with the remaining 11 pairs considered improbable but worth following up. Two previously identified clusters by us possibly host classical Cepheids (OC-0125/V1788 Cyg and OC-0675/OGLE-BLG-CEP-114). In addition, we identify 38 new open cluster candidates within the Galactic disk.

Key words. Galaxy: stellar content – open clusters and associations: general – stars: variables: Cepheids – methods: data analysis

1. Introduction

Classical Cepheids are intermediate-mass stars that can exhibit regular pulsations in fundamental and overtone modes, and possess ages that overlap with those of open clusters (OCs; see Table A.1). Therefore, classical Cepheids are expected to be in OCs, and such pairs are significant objects in astronomy.

Cepheids have a famous period–luminosity relationship (PLR), also known as the Leavitt law, securing them as standard candles for constituting the cosmic distance scale and as essential indicators, empowering firmer constraints on Hubble’s law (e.g., Leavitt & Pickering 1912; Feast 1999; Madore & Freedman 1991). However, one of the critical debates in cosmology is the Hubble constant (H_0) tension. Based on the current standard Λ cold dark matter (Λ CDM) model, estimates of H_0 based on measurements of fluctuations in the temperature and polarization of the cosmic microwave background (CMB) from Planck and ACT+WMAP consistently yield values of 67.4 ± 0.5 and 67.6 ± 1.1 km s⁻¹ Mpc⁻¹, respectively (Planck Collaboration et al. 2020; Aiola et al. 2020). In contrast, Riess et al. (2019, 2021) argued that the Cepheid distance scale implies a larger value of $H_0 = 73.2 \pm 1.3$ km s⁻¹ Mpc⁻¹, in tension with the CMB result. Using the tip of the red giant branch in the Large Magellanic Cloud, the Carnegie-Chicago Hubble Program put forward an $H_0 = 69.6 \pm 1.9$ km s⁻¹ Mpc⁻¹, close to the CMB prediction considering the uncertainty (Freedman et al. 2019, 2020). Likewise, Majaess (2020) pointed out that the accuracy of Cepheid distances may be swayed by neglected or inaccurate blending corrections for remote targets, which would result in an overestimated H_0 . Therefore, it is not clear so far whether the H_0 tension means new physics are needed for the Λ CDM model or that unknown systematic errors exist in the above measurements. Open cluster–Cepheid pairs can help to solve this problem. As a large number of cluster members makes it possible to derive more accurate astronomical parameters than those of individual sources, OCs harboring Cepheids can optimize the zero point of

the PLR for Cepheids, and ultimately contribute to reducing the H_0 uncertainty by providing a Galactic calibration of the Leavitt law (e.g., Turner & Burke 2002; Chen et al. 2017; Breuval et al. 2020). Recently, using only 17 reported cluster Cepheids with *Hubble Space Telescope* photometry and *Gaia* Early Data Release 3 (EDR3) parallax, Riess et al. (2022) constrained the PLR of Cepheids and obtained a 5%–7% reduction in the H_0 uncertainty.

Open cluster–Cepheid pairs are important in additional ways. First, cluster Cepheids can be used to benchmark *Gaia* parallax, especially for distant Cepheids. *Gaia* parallax is affected by a systematic error, the so-called “parallax zero point”, which was first clearly identified in Data Release 2 using quasars (Gaia Collaboration et al. 2018; Lindegren et al. 2018). Also, OC–Cepheid pairs could be an important diagnostic tool for examining the *Gaia* parallax offset, whereby the cluster distance is tied to more stars of perhaps a different mean color than the Cepheid, and offsets can be examined as a function of direction, magnitude, color, and distance. For an ongoing investigation using cluster Cepheids to assess the systematic errors in the *Gaia* data, we recommend Riess et al. (2022). Second, cluster Cepheids are expected to benchmark the stellar evolution models and theoretical isochrones (e.g., Bono et al. 2005; Turner et al. 2006). Third, OC–Cepheid pairs can be of service in elucidating the pulsating nature and dynamical evolution of Cepheids (e.g., Fry & Carney 1997; Lemasle et al. 2017; Dinnbier et al. 2022). In addition, Cepheids adhere to a period–age relation (PAR), whereby longer period Cepheids are more luminous and massive (e.g., Efremov 2003; Bono et al. 2005; Turner et al. 2012a). Therefore, the ages of OC–Cepheid pairs based on isochrone fitting to the cluster colour–magnitude diagrams (CMDs) can be used to calibrate the PAR of Cepheids (e.g., Efremov 2003; Anderson et al. 2016; De Somma et al. 2020). As both OCs and Cepheids are young objects, they can also be used as good tracers for studying spiral arms and the detailed disk structure of the Milky Way (e.g., Chen et al. 2019; Hao et al. 2021; Poggio et al. 2021). In partic-

ular, [Minniti et al. \(2020\)](#) used classical Cepheids to trace the gradient of metallicity on both sides of the Galactic disk.

Taking advantage of the *Gaia* data, [Hao et al. \(2020, 2022\)](#) found more than 700 new OC candidates. Although over 2000 new OCs have been identified, the Galactic OC census is considered to be far from complete and this particularly true along heavily obscured sightlines (e.g., [Cantat-Gaudin et al. 2020; Castro-Ginard et al. 2022](#)). Thanks to the VISTA variables in the Vía Láctea survey and other longer wavelength surveys, classical Cepheids are being discovered on the other side of the Galaxy (e.g., [Dékány et al. 2015b; Minniti et al. 2021](#)). At present, more than 3000 classical Cepheids have been discovered in the Milky Way (e.g., [Chen et al. 2020; Pietrukowicz et al. 2021](#)).

Despite the significance of OC–Cepheid pairs and the discovery of thousands of OCs and classical Cepheids, only a few OCs harboring Cepheids have been reported so far. The presence of Cepheids in Galactic OCs was first discovered by [Doig \(1925, 1926\)](#) and probably others, as noted by [Fermie \(1969\)](#). By cross-matching the known OCs in *Gaia* with a list of Cepheids, [Zhou & Chen \(2021\)](#) reported the largest OC–Cepheid sample to date, in which only 33 Cepheids exist in 29 OCs. Therefore, the identification of more OC–Cepheid pairs is an indispensable undertaking with great importance.

The latest *Gaia* data release, DR3, includes astrometric and photometric measurements of 1.8 billion objects, and the determination of the mean radial velocity (RV) of 33 million objects ([Gaia Collaboration et al. 2022b](#)). Meanwhile, the data quality of *Gaia* has been further improved. Previous studies identifying OC–Cepheid pairs mainly cross-matched Cepheids with known OCs. However, as mentioned above, the OC census of the Milky Way is incomplete. Hence, based on the aforementioned comprehensive datasets, this work aims to find OC–Cepheid pairs in the regions of Cepheids using the cluster-search method employed in our previous studies ([Hao et al. 2020, 2022](#)).

We organize this paper as follows. The data used in this work are described in Sect. 2. Section 3 presents the method applied to the search for OCs holding classical Cepheids. The results are displayed in Sect. 4 and we summarize this work in Sect. 5.

2. Data

The classical Cepheids adopted in this work come from the catalog compiled by [Pietrukowicz et al. \(2021\)](#), who carefully inspected candidate Cepheids from many surveys based on their long-term experience in the field of variable stars. The surveys related to the sources in this catalog are as follows: General catalog of Variable Stars, All Sky Automated Survey, Northern Sky Variability Survey, Optical Gravitational Lensing Experiment, Asteroid Terrestrial–impact Last Alert System, All–Sky Automated Survey for Supernovae, Wide–field Infrared Survey Explorer, *Gaia* astrometric mission, VISTA Variables in the Via Lactea, Zwicky Transient Facility, and so on (for more details, see [Pietrukowicz et al. 2021](#), and references within). This catalog, with a purity exceeding 97%, contains a total of 3 352 classical Cepheid variables, which are available at the OGLE Internet Data Archive¹. In addition, [Pietrukowicz et al. \(2021\)](#) not only presented detailed information on these classical Cepheids but also cross-matched them with the *Gaia* EDR3 catalog. In this work, considering that the present-day uncertainty on parallax in

the *Gaia* area can reach 0.02–0.03 mas ([Lindegren et al. 2021](#)), we decided to mainly concentrate on the objects within 5 kpc of the Sun, resulting in a subsample that contains 1 085 classical Cepheids. For each of these Cepheids, we have obtained detailed information such as astrometric and photometric parameters in the *Gaia* DR3 dataset.

We used the dataset from the *Gaia* DR3 catalog, which can be found at the *Gaia* archive². The astrometric and photometric parameters of stars in *Gaia* DR3 are the same as those in *Gaia* EDR3 ([Gaia Collaboration et al. 2020](#)), which contain stellar celestial positions, parallaxes, proper motions (l , b , ϖ , μ_{α^*} , and μ_{δ}), and three photometric bands (G , G_{BP} , and G_{RP}). Meanwhile, *Gaia* DR3 includes 33 million objects with new determinations on their mean radial velocities. As in many previous works searching for OCs (e.g., [Cantat-Gaudin et al. 2018; Hao et al. 2022; Castro-Ginard et al. 2022](#)), we only chose sources brighter than $G = 18$. For sources with five-parameter solutions at this magnitude, the median parallax uncertainty on them is 0.120 mas, and the median uncertainties on proper motions in μ_{α^*} and μ_{δ} are 0.123 and 0.111 mas yr⁻¹, respectively ([Lindegren et al. 2021](#)). We also rejected sources that present negative parallaxes or large proper motions with $|\mu_{\alpha^*}|, |\mu_{\delta}| > 30$ mas yr⁻¹. As the aim of this work is to find OCs containing classical Cepheids, we only focus on the 1 085 spatial regions where selected Cepheids are present; our experimental setup is described in the following section.

3. Methods

The sample-based clustering search method was successfully adopted in our previous studies and we found more than 700 new OC candidates in the *Gaia* area ([Hao et al. 2020, 2022](#)). This method consists primarily of four steps: determining spatial regions, searching for stellar clusters in the five-dimensional (5D) parametric space (l , b , ϖ , μ_{α^*} , and μ_{δ}), selecting targets based on proper-motion dispersion, and visually inspecting the multiple distributions. In this section, we describe the method and process of searching for OCs containing classical Cepheids.

Sample determination. Under the selection criteria of stars described in Sect. 2, we first extracted stars around the spatial locations of classical Cepheids. The key aspect of this step is to decide the spatial size and distance boundaries of the different regions where Cepheids exist. In this work, by referencing our previous experience in searching for OCs ([Hao et al. 2020, 2022](#)), the celestial sizes and distance boundaries of different spatial regions are set in the range of $[1^\circ, 10^\circ]$ and $[0.5, 5]$ kpc, respectively, mainly according to the distances of classical Cepheids and the spatial density of regions. Thus, we obtained 1 085 original stellar samples. In addition, if in the following search there are star clusters located at the borders of regions, we change the sizes of the regions and re-detect these star clusters.

Clustering algorithm. The powerful unsupervised clustering algorithm, known as the density-based spatial clustering of applications with noise (DBSCAN, [Ester et al. 1996](#)), was applied in the multidimensional space (i.e., l , b , ϖ , μ_{α^*} , and μ_{δ}) to find spatial over-density structures in the regions. For DBSCAN, the parameters ϵ and $minPts$ are needed, which specify the radius of a neighborhood with respect to some point and the desired minimum cluster size, respectively. We let the parameter $minPts$ vary in the range of six to ten stars. The corresponding parameters ϵ of each sample were then automatically calculated using the z-score standardization, a Gaussian

¹ <https://www.astrouw.edu.pl/ogle/ogle4/OCVS/allGalCep.listID>

² <https://gea.esac.esa.int/archive/>

kernel-density-estimation method (Lampe et al. 2011), and the k-nearest ($k = \min(Pts-1)$) neighbors algorithm (Altman 1992); see Hao et al. (2020) for elaborate details on the determination of ϵ . After preparing the parameter pairs for all samples, we conducted the search for statistical stellar clusters in all regions of existing classical Cepheids.

We noticed that there are some classical Cepheids located close to each other in spatial locations, which means regional overlaps exist among some initial samples, resulting in several stellar clusters being found repeatedly. We resolved this case by identifying those stellar clusters that have comparable mean parameters within $3\sigma_i$ (σ is the standard deviation, $i = l, b, \varpi, \mu_{\alpha^*}$, and μ_δ) in the 5D parametric space. Subsequently, we visually inspected these stellar clusters and filtered out the repetitions.

Selection based on proper-motion dispersion. The apparent proper-motion dispersion of a stellar cluster can serve as an effective means to distinguish reasonable OCs from implausible ones, and this technique has been used in some work to select potentially real OCs from spatial over-density structures (e.g., Hunt & Reffert 2021; Hao et al. 2022). The gravitationally bound OC systems generally have small internal velocity dispersions. Here, as in our previous work (Hao et al. 2022), we selected the possibly genuine OCs using the following proper-motion criterion:

$$\sqrt{\sigma_{\mu_{\alpha^*}}^2 + \sigma_{\mu_\delta}^2} \leq \begin{cases} 0.5 \text{ mas yr}^{-1} & \text{if } \varpi < 1 \text{ mas} \\ 2\sqrt{2}\frac{\varpi}{4.7404} \text{ mas yr}^{-1} & \text{if } \varpi \geq 1 \text{ mas} \end{cases} \quad (1)$$

Here, $\sigma_{\mu_{\alpha^*}}$, σ_{μ_δ} , and ϖ are the standard deviations of two proper motions and the mean parallax of statistical stellar clusters. For the property of proper-motion dispersions of OCs identified in the *Gaia* area, we recommend Cantat-Gaudin & Anders (2020).

Visual inspection and confirmation. For the potentially real OCs, we visually inspected their multiple characters, such as their members, the density relative to the background stellar distribution, the distribution of radial velocities when available, and especially the CMDs. As the member stars of an OC are almost simultaneously formed in the same molecular cloud, their distribution on the CMD can exhibit the feature of some empirical isochrone. These measures were mainly taken for the potentially genuine OCs that have not been reported to select the more reliable OC candidates.

We computed the mean RV , and the weighted standard deviation of RV for each OC candidate using the method described in Soubiran et al. (2018). We also estimated the ages, line-of-sight extinction (absorption, A_G), and distance modulus (DM) of the proposed OC candidates using the photometric parameters (G , G_{BP} , and G_{RP}) provided in *Gaia* to construct the theoretical isochrones in their CMDs. It should be noted that the differential reddening seen in some OCs can complicate matters considerably, in that a tight obvious main sequence and evolved pattern may not be seen. In this case, differential reddening procedures need to be employed, potentially using a color-color diagram (e.g., Turner 1994, see Figure 2 and Figure 3 for NGC 1545). The isochrones we adopted are derived from the PARSEC library (Bressan et al. 2012), which has been updated for the *Gaia* passbands with the photometric calibration of Evans et al. (2018) and contains logarithmic ages (i.e., $\log(\text{age}/\text{yr})$) ranging from 5.92 to 10.13 and metal fractions (z) ranging from 0.015 to 0.029, as well as a series of isochrones that are generated with steps of $\Delta\log(\text{age}/\text{yr}) = 0.02$ and $\Delta z = 0.001$. We used the least square fitting method to obtain an isochrone that is as reliable as possible for each OC candidate. Meanwhile, the extinction and reddening that we adopted are corrected using an extinction law

of $R_v = 3.1$ (O'Donnell 1994) for the Milky Way galaxy, and the applied approximate relation is $E(G_{BP} - G_{RP}) = 0.50 A_v$ as recommended by Andrae et al. (2018). We refer the reader to Sect. 3.4 in Hao et al. (2022) for more details on the determinations.

4. Results

After implementing the processes described in Sect. 3, we cross-matched the stellar clusters found in this work with reported OCs to identify the OCs that are already known and those that are new findings. In total, 635 known OCs were re-detected, and we proposed 38 stellar clusters as newly found OC candidates. The classical Cepheids used in this work were cross-matched with the above OCs, and we found 45 OCs harboring a total of 50 Cepheids. For the newly found OCs, we determined their parameters and investigated their characteristics.

4.1. Cross-matching with known OCs

The stellar clusters found in this work were first cross-matched with previously reported OCs in the *Gaia* area: Cantat-Gaudin et al. (2018), Castro-Ginard et al. (2018), Cantat-Gaudin et al. (2019), Castro-Ginard et al. (2019), Castro-Ginard et al. (2020), Sim et al. (2019), Liu & Pang (2019), Ferreira et al. (2019), Ferreira et al. (2020), Ferreira et al. (2021), Hao et al. (2020), He et al. (2021), Hunt & Reffert (2021), Hao et al. (2022), and Castro-Ginard et al. (2022). In general, two stellar clusters can be considered a match if their mean parameters are within $3\sigma_i$ ($i = l, b, \varpi, \mu_{\alpha^*}$ and μ_δ) in the 5D parametric space. Thus, in this step, we obtained 594 previously known OCs in the *Gaia* data.

Subsequently, stellar clusters obtained by us were cross-matched with OCs that were known before *Gaia*, which mainly derive from the catalogs compiled by Dias et al. (2002, V3.5, 2015 edition) and Kharchenko et al. (2013), which contain approximately 2000 and 3000 objects, respectively, while they have repetitive sources. The criterion used in this step is the same as in our previous work (Hao et al. 2022). We first selected star clusters that fall within a circle of 0.5° radii of objects listed in these two catalogs. If the mean proper motions (μ_{α^*} and μ_δ) of the listed objects are within three times the standard deviations of the stellar clusters found in this work, and their distances are compatible, they can be considered matched. Here, the distance of a star cluster found in this work is the inverse of the mean parallax, and the corresponding error comes from three times the standard deviation of the parallax. Cantat-Gaudin et al. (2018) took into account many objects in these two catalogs, but we re-detected 24 known OCs in Dias et al. (2002) and 21 known OCs in Kharchenko et al. (2013), respectively, and 4 OCs among them are repetitive. Similar to the OC catalogs, we also cross-matched our findings to the globular cluster catalog reported by Baumgardt et al. (2019), but we did not explore any coincidences.

For the remaining stellar clusters found in this work that were not yet cross-matched with known OCs, we carefully inspected their multidimensional nature as described in Sect. 3 and proposed 38 reliable ones to be OC candidates, which are numbered from OC-0705 in order to be the continuation of our previous work (Hao et al. 2022). Combining these 38 newly found OC candidates with 594 OCs in *Gaia* and 41 OCs in the catalogs before *Gaia*, we searched for a total of 673 OCs in this work. Subsequently, we investigated these OCs to identify OCs hosting classical Cepheids.

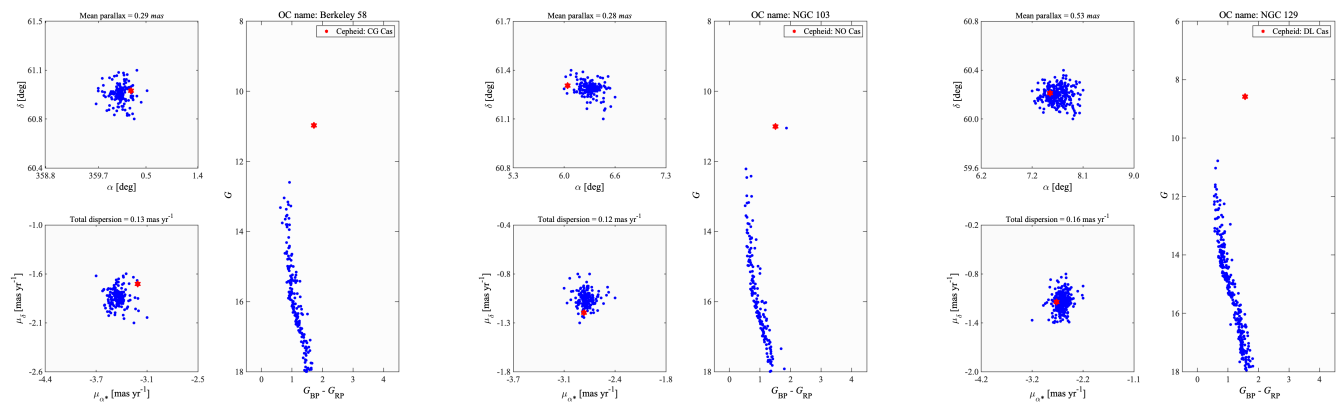


Fig. 1. Examples of OCs (blue dots) harboring classical Cepheids (red hexagram). The columns of each panel represent the distributions of the member stars of OCs and classical Cepheids for position in RA (α) and Dec (δ), proper motions in μ_{α^*} and μ_{δ} , and the CMD in G vs. $G_{BP} - G_{RP}$, as well as the mean parallax and total proper-motion dispersion of OCs. Here, the listed OCs are Berkeley 58, NGC 103, and NGC 129.

4.2. Open clusters housing classical Cepheids

We regarded OCs and classical Cepheids as combinations in two scenarios: Cepheids are member stars of OCs; or the 5D astrometric parameters (l , b , ϖ , μ_{α^*} , and μ_{δ}) of Cepheids and OCs are concordant within three times the corresponding standard deviations. As described in Sect. 2, we obtained *Gaia* DR3 source_id for each classical Cepheid. For the first case, we cross-matched the list of classical Cepheids with the member stars of the 673 OCs found in this work. The cross-match was performed using *Gaia* DR3 source_id and returned 30 OCs holding 32 Cepheids. The 5D astrometric parameters of the remaining classical Cepheids were then compared with all found OCs, resulting in 18 Cepheids associated with 18 OCs, of which 3 OCs are the same ones as above. Thus, we identified 45 OCs housing 50 classical Cepheids, and the names of these OC-Cepheid pairs are listed in Table A.1 in the Appendix.

We cross-matched the OC-Cepheid pairs found in this work with those in Zhou & Chen (2021), who reported the discovery of 29 OCs containing 33 Cepheids. Finally, we were able to re-detect 27 OCs holding 30 Cepheids. We noticed that the differences in proper motion in μ_{δ} between the remaining two OCs (Ruprecht 97 and UBC 375) and their two associated classical Cepheids proposed by Zhou & Chen (2021) are significantly large (10.9σ and 7.3σ , respectively), resulting in the two pairs not being identified in this work. There is another Cepheid (V379 Cas) not being matched by us because its spatial location is about one degree away from the target OC (NGC 129) in the sky. The dynamical evolution proposed by Turner (1985) suggests that instances of Cepheids may be possible members of cluster coroneae. Coulson & Caldwell (1985) and Majaess et al. (2013) both reported that the Cepheid QZ Nor is a coronal member of the OC NGC 6067. Therefore, the Cepheid V379 Cas may be an ejected member of the NGC 129 cluster. Although V379 Cas is not followed up here, it is still worth investigating. We also recovered some interesting OCs that contain more than one classical Cepheid: for example, the widely known Galactic OC NGC 7790 hosting three Cepheids, and the OC Kronberger 84 holding two Cepheids reported by Zhou & Chen (2021). The cross-match using *Gaia* DR3 source_id shows that the Cepheid V733 Cyg is a non-member of Kronberger 84, but that the 5D astrometric parameters of V733 Cyg are consistent with the cluster, within three times the corresponding standard deviations.

For the 45 OCs containing classical Cepheids, 35 are previously known OCs compiled by Cantat-Gaudin et al. (2020), two OCs (OC-0125 and OC-0675) were reported by Hao et al. (2022), one OC (Alessi 95) was reported by Turner et al. (2012b) and Majaess et al. (2012), one OC (UBC 1424) was reported by Castro-Ginard et al. (2022), and the last six are newly discovered in this work. Based on the member stars of the 45 OCs in *Gaia* DR3, we determined their mean astrometric parameters (α , δ , ϖ , μ_{α^*} , and μ_{δ}) and the corresponding standard deviations, as presented in Table A.1. The apparent angular radius (θ) of each OC was estimated as the square root of the quadratic sum of σ_l and σ_b (e.g., Castro-Ginard et al. 2020; Hao et al. 2022; Castro-Ginard et al. 2022). The cluster apparent diameters are then determined as two times the θ . The ages and uncertainties of the known OCs are from the previous determinations in Sana et al. (2010), Turner et al. (2012b), Cantat-Gaudin et al. (2020), Hao et al. (2022), and Castro-Ginard et al. (2022), and those of newly found OCs were estimated by the method described in Sect. 3. Table A.1 also presents the astrometric parameters (α , δ , ϖ , μ_{α^*} , and μ_{δ}) of Classical Cepheids, which are from the dataset of *Gaia* DR3, and the listed periods of Cepheids are from Pietrukowicz et al. (2021). The Cepheid ages listed in Table A.1 are taken from the mean calculation of the Cepheid PAR reported in following three works: Efremov (2003), Bono et al. (2005), and Turner et al. (2012a), and the deviation is cited as the uncertainty. We note that Efremov (2003) and Bono et al. (2005) only present the PAR for fundamental and first-overtone classical Cepheids, and so the second-overtone pulsating mode of the Cepheid OGLE-GD-CEP-1673 means that its age is unavailable from the two works, and its age uncertainty is not listed in Table A.1. However, it should be noted that the obtained ages of Cepheids are uncertain parameters, and are affected by reddening, distance, photometric calibrations, and so on, as pointed out by Bono et al. (2005). We also estimated the angular separation between the classical Cepheid and its host OC, where the cluster centre is derived from the mean astrometric positions of member stars.

We noticed that some OCs may exhibit pre-main sequence (PMS) characteristics, and therefore would be unrelated to Cepheids, particularly the lower period ones. For example, the readily discernible PMS of Trumpler 14 was studied by Sana et al. (2010), and the presence of O-type stars in NGC 6193 was reported by Skinner et al. (2005), suggesting that the two

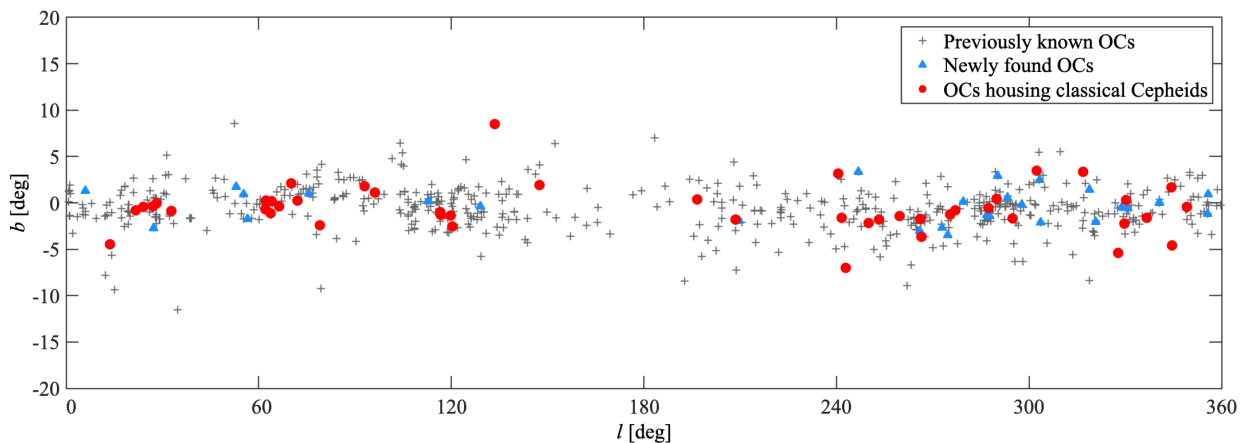


Fig. 2. Distributions in Galactic coordinates of the OCs housing classical Cepheids (red dots), newly found OCs (blue triangles) and previously known OCs (black plus) obtained in this work.

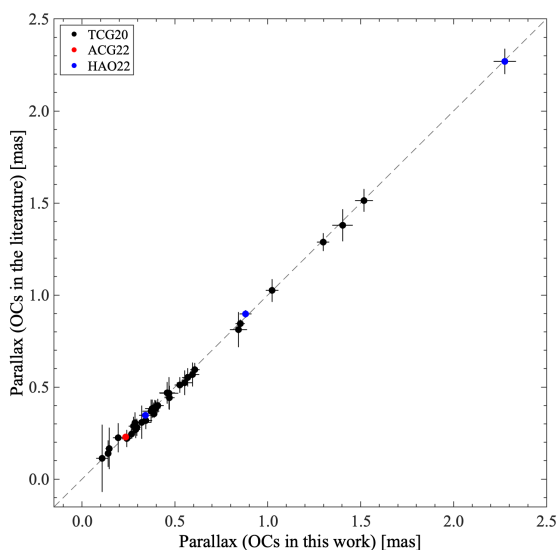


Fig. 3. Parallactic comparison between OCs containing classical Cepheids found in this work and those previously reported in Cantat-Gaudin et al. (2020, TCG20), Castro-Ginard et al. (2022, ACG22), and Hao et al. (2022, HAO22)

OCs are not related to Cepheids. Indeed, OCs with ages younger than ten million years are unlikely to be related to Cepheids, and those with ages near ten million years also tend to be related to very long-period Cepheids (e.g., Anderson et al. 2016). We investigated all the identified OC–Cepheid pairs by considering the OC ages and the periods of Cepheids, and found that 11 Cepheids may be unrelated to OCs. However, it is interesting that the astrometric matches of these Cepheids and their host OCs still emerge, and so these Cepheids are worthy of follow-up investigation in order to come to a firm conclusion on their nature. In Table A.1, class A Cepheids are related to OCs and have been identified as cluster members, Cepheids in class B are related to OCs but have not been identified as cluster members, and class C Cepheids may be unrelated to OCs but they possess similar astrometric parameters. Table A.1 can be found online at the CDS, together with the table reporting the member stars of OCs harboring classical Cepheids.

Figure 1 shows three examples of OCs holding classical Cepheids, including the members of OCs and Cepheids in the astrometric spaces as well as CMDs. The remaining cases are

presented in Figure A.1 in the Appendix. As intermediate-mass stars, classical Cepheids have evolved away from the main sequence and are in the stage of shell hydrogen burning or core helium burning (e.g., Turner et al. 2006). Hence, in the CMDs of bona fide OCs harboring classical Cepheids, Cepheids are generally located on the classical instability strip and are brighter than the main sequence stars. We visually inspected the CMDs of the OC–Cepheid pairs identified in this work and found 38 Cepheids with the above features. For the last 12 classical Cepheids that may not be on the classical instability strip of their host OCs, these classical Cepheids require further investigation, and we associated asterisks with the names of these classical Cepheids in Table A.1.

Figure 2 presents the distribution of the 45 OCs hosting classical Cepheids in Galactic l and b coordinates. The vast majority ($\sim 93\%$) of them are located within the Galactic disk at latitudes of $|b| \leq 5^\circ$. We also made a comparison between the parallaxes of OCs containing classical Cepheids found in this work and those previously reported in Cantat-Gaudin et al. (2020), Castro-Ginard et al. (2022), and Hao et al. (2022), as shown in Fig. 3. The mean parallaxes of the known OCs re-detected in this work are in good agreement with previously published values. However, compared with the previous results, the smaller errors of parallaxes obtained here demonstrate the improved data quality of *Gaia* DR3 over *Gaia* data release 2. We also noticed that 43 of these OCs have RV measurements, of which 40 are based on more than one member star, and 35 are based on more than two member stars. The OCs marked with asterisks in Table A.1 have an RV measurement. Therefore, in addition to providing useful indications for optimizing the zero-point of the Cepheid period–luminosity relationship and period–age relation, it is hopeful that these OCs can be used to unveil the nature and especially the dynamical evolution of classical Cepheids.

4.3. Newly found OCs

As described in Sect. 4.1, aside from re-detecting 635 previously known OCs, we are fortunate to propose 38 reliable ones as new OC candidates in this work. Figure 4 displays the distributions of some examples of newly found OCs. Here we present the features of their member stars in astrometric spaces and CMDs, indicating that these proposed new OCs show high concentrations of member stars in the five astrometric parameters, and the members in the CMDs are concentrated on potentially theoretic-

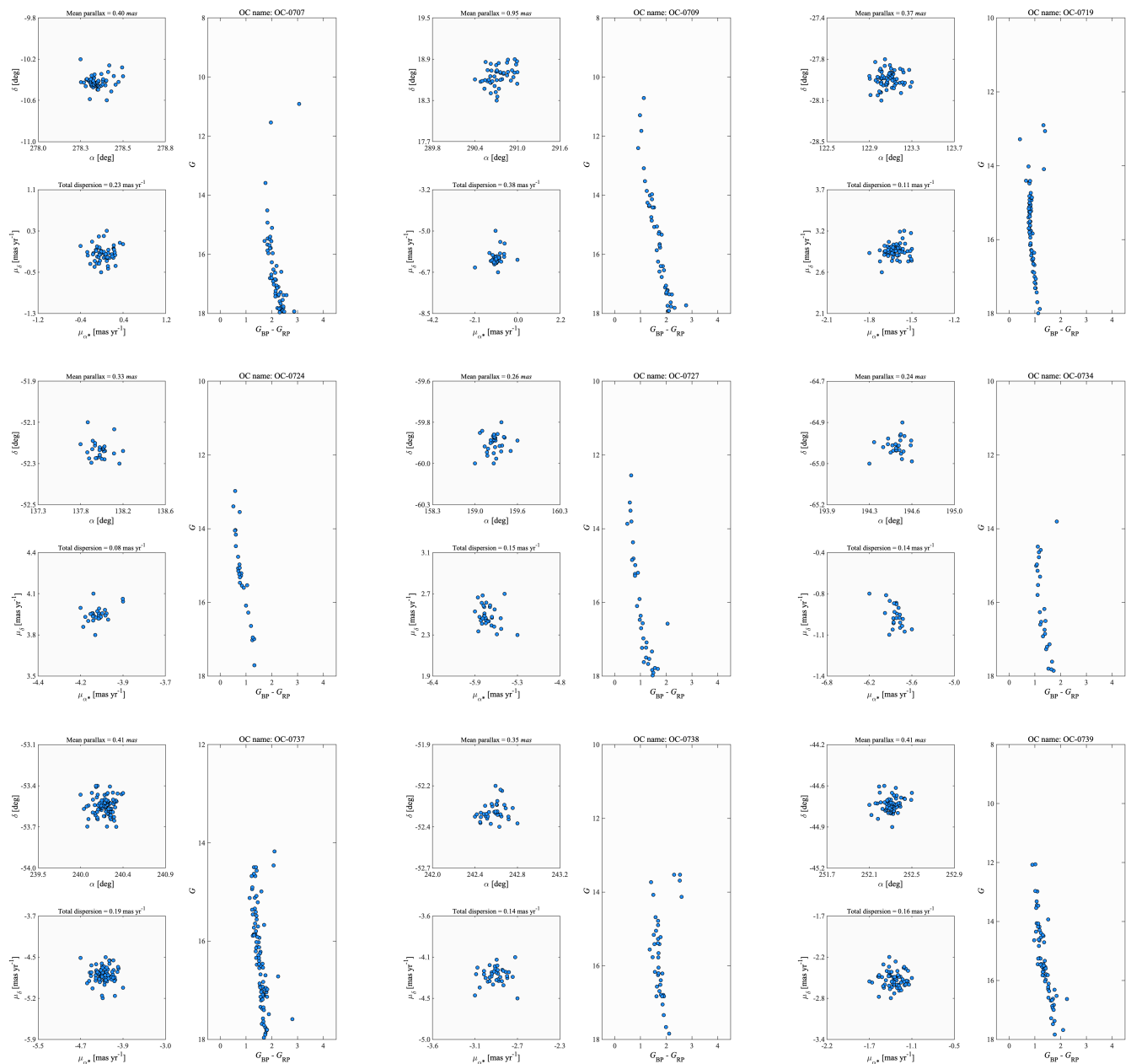


Fig. 4. Examples of newly found OCs in this work. The columns of each panel are the same as Figure 1. Here, the listed OCs are OC-0707, OC-0709, OC-0719, OC-0724, OC-0727, OC-0734, OC-0737, OC-0738, and OC-0739.

cal isochrones. Table A.2 of the Appendix contains a list of the parameters of the new OC candidates, including their mean astrometric parameters (α , δ , l , b , ϖ , μ_{α^*} , and μ_{δ}) and standard deviations, RV s, and the weighted standard deviations of RV s when available, as well as the estimated ages, line-of-sight extinction (A_G), and DM. In addition, the apparent angular sizes of these new OC candidates were computed as the square root of the quadratic sum of σ_l and σ_b following Castro-Ginard et al. (2020), Hao et al. (2022), and Castro-Ginard et al. (2022). The table can be found online at the CDS, including the table of member stars.

The new OC candidates are generally at larger distances, of which $\sim 95\%$ are further than 1 kpc, and only two OCs are located within 1 kpc. For the newly found OCs, 31 of them have member stars with RV s in *Gaia* DR3, more than half of which

contain more than one star with an RV measurement, and the names of these OCs have been placed with asterisks in Table A.2. The distributions of these OCs in the Galactic plane are also shown in Fig. 2. The newly found OCs are mostly found at low latitudes within the Galactic disk, with the vast majority of new OC candidates ($\sim 97\%$) located at $|b| \leq 4^\circ$, and only one at $b \approx 7^\circ$.

5. Summary

Combining the high-precision data provided by *Gaia* DR3 and known classical Cepheids with our previously practiced clustering search method, we conducted a search for OCs containing classical Cepheids. We identified 50 classical Cepheids associated with 45 OCs in 5D astrometric space. After investigating the

ages of the OCs and the periods of the Cepheids, we found 39 OC-Cepheid pairs to be probable, and a remaining 11 Cepheids to be improbable and possibly unrelated to OCs but worthy of follow-up investigation. For all of these OC–Cepheid pairs, we provide their astrometric and astrophysical parameters. In addition to re-detecting 635 known OCs in the literature, we also propose 38 newly found OC candidates within the Galactic disk based on a detailed inspection of the multidimensional distributions of their member stars. For each of these new OC candidates, we present its mean astrometric values and radial velocity when available, together with estimations of age, line-of-sight extinction, and distance modulus. The new OCs are generally located at greater distances from the Sun, which can help to improve the completeness of the Galactic OC census.

Our current search mainly focuses on the regions within 5 kpc of the Sun. Hence, it is expected that more OC–classical Cepheid pairs will be detected in our Galaxy along with the improvements in parallax and proper motion precision of the future data releases of *Gaia*.

Acknowledgements

We sincerely appreciate the anonymous referee for the instructive comments which help us to improve the paper. This work was funded by NSFC Grants 11933011, 11873019, 12203104, and the Key Laboratory for Radio Astronomy. YJL thanks support from the Natural Science Foundation of Jiangsu Province (grant number BK20210999) and the Entrepreneurship and Innovation Program of Jiangsu Province. Our work has made use of data from the European Space Agency (ESA) mission *Gaia* (<https://www.cosmos.esa.int/gaia>), processed by the *Gaia* Data Processing and Analysis Consortium (DPAC, <https://www.cosmos.esa.int/web/gaia/dpac/consortium>). Funding for the DPAC has been provided by national institutions, in particular the institutions participating in the *Gaia* Multilateral Agreement.

References

Aiola, S., Calabrese, E., Maurin, L., et al. 2020, *JCAP*, 2020, 047
 Altman, N. S. 1992, *BAN*, 46, 175
 Anderson, R. I., Saio, H., Ekström, S., Georgy, C., Meynet, G. 2016, *A&A*, 591, A8
 Andrae, R., Fouesneau, M., Creevey, O., et al. 2018, *A&A*, 616, A8
 Baumgardt, H., Hilker, M., Sollima, A., & Bellini, A. 2019, *MNRAS*, 482, 5138
 Bono, G., Marconi, M., Cassisi, S., et al. 2005, *ApJ*, 621, 966
 Bressan, A., Marigo, P., Girardi, L., et al. 2012, *MNRAS*, 427, 127
 Breuval, L., Kervella, P., Anderson, R. I., et al. 2020, *A&A*, 643, A115
 Cantat-Gaudin, T., Jordi, C., Vallenari, A., et al. 2018, *A&A*, 618, A93
 Cantat-Gaudin, T., Krone-Martins, A., Sedaghat, N., et al. 2019, *A&A*, 624, A126
 Cantat-Gaudin, T., Anders, F., Castro-Ginard, A., et al. 2020, *A&A*, 640, A1
 Cantat-Gaudin, T., & Anders, F. 2020, *A&A*, 633, A99
 Castro-Ginard, A., Jordi, C., Luri, X., et al. 2018, *A&A*, 618, A59
 Castro-Ginard, A., Jordi, C., Luri, X., Cantat-Gaudin, T., & Balaguer-Nunez, L. 2019, *A&A*, 627, A35
 Castro-Ginard, A., Jordi, C., Luri, X., et al. 2020, *A&A*, 635, A45
 Castro-Ginard, A., Jordi, C., Luri, X., et al. 2022, *A&A*, 661, A118
 Chen, X., de Grijs, R., Deng, L., 2017, *MNRAS*, 464, 1119
 Chen, X., Wang, S., Deng, L., et al. 2019, *NatAs*, 3, 320
 Chen, X., Wang, S., Deng, L., et al. 2020, *ApJS*, 249, 18
 Coulson, I. M., & Caldwell, J. A. R. 1985, *MNRAS*, 216, 671
 De Somma, G., Marconi, M., Cassisi, S., et al. 2020, *MNRAS*, 496, 5039
 Dékány, I., Minniti, D., Majaess, D., et al. 2015b, *ApJ*, 812, L29
 Dias, W. S., Alessi, B. S., Moitinho, A., & Lépine, J. R. D. 2002, *A&A*, 389, 871
 Dinnbier, F., Anderson, R. I., & Kroupa, P. 2022, *A&A*, 659, A169
 Doig, P. 1925, *JBAA*, 35, 202
 Doig, P. 1926, *JBAA*, 36, 60
 Efremov, Y. N. 2003, *AREP*, 47, 1000

Ester, M., Kriegel, H.-P., Sander, J., & Xu X. 1996, 2nd International Conference on Knowledge Discovery and Data Mining (AAAI Press), 96, 226
 Evans, D. W., Riello, M., De Angeli, F., et al. 2018, *A&A*, 616, A4
 Feast, M. W. 1999, *PASP*, 111, 775
 Ferreira, A. F., Santos, J. F. C., Corradi, W. J. B., Maia, F. F. S., & Angelo, M. S. 2019, *MNRAS*, 483, 5508
 Ferreira, A. F., Corradi, W. J. B., Maia, F. F. S., Angelo, M. S., & Santos, J. F. C. 2020, *MNRAS*, 496, 2021
 Ferreira, A. F., Corradi, W. J. B., Maia, F. F. S., Angelo, M. S., & Santos, J. F. C. 2021, *MNRAS*, 502, L90
 Fernie, J. D. 1969, *PASP*, 81, 707
 Freedman, W. L., Madore, B. F., Hatt, D., et al. 2019, *ApJ*, 882, 34
 Freedman, W. L., Madore, B. F., Hoyt, T., et al. 2020, *ApJ*, 891, 57
 Fry, A. M., & Carney, B. W. 1997, *AJ*, 113, 1073
Gaia Collaboration (Brown, A. G. A., et al.) 2018, *A&A*, 616, A1
Gaia Collaboration (Brown, A. G. A., et al.) 2020, *A&A*, 649, A1
Gaia Collaboration (Vallenari, A., et al.) 2022, *A&A*, accepted
 Hao, C. J., Xu, Y., Wu, Z. Y., et al. 2020, *PASP*, 132, 034502
 Hao, C. J., Xu, Y., Hou, L. G., et al. 2021, *A&A*, 652, A102
 Hao, C. J., Xu, Y., Wu, Z. Y., et al. 2022, *A&A*, 660, A4
 He, Z. H., Xu, Y., Hao, C. J., Wu, Z. Y., & Li, J. J. 2021, *Res. Astron. Astrophys.*, 21, 093
 Hunt E. L., & Reffert S. 2021, *A&A*, 646, A104
 Kharchenko, N. V., Piskunov, A. E., Schilbach, E., Röser, S., & Scholz, R.-D. 2013, *A&A*, 558, A53
 Lampe, O. D., & Hauser, H. 2011, 2011 IEEE Pacific Visualization Symp. (Piscataway, NJ: IEEE), 171
 Leavitt H. S., & Pickering E. C. 1912, *Harv. Coll. Obs. Circ.*, 173, 1
 Lemasle, B., Groenewegen, M. A. T., Grebel, E. K., et al. 2017, *A&A*, 608, A85
 Lindegren, L., Hernandez, J., Bombrun, A., et al. 2018, *A&A*, 616, A2
 Lindegren, L., Klioner, S. A., Hernández, J. et al. 2021a, *A&A*, 649, A2
 Liu, L., & Pang, X. 2019, *ApJS*, 245, 32
 Majaess, D. J., Turner, D. G., Gallo, L., et al. 2012, *ApJ*, 753, 144
 Majaess, D. J., Sturch, L., Moni Bidin, C., et al. 2013, *Ap&SS*, 347, 61
 Majaess, D. J. 2020, *ApJ*, 897, 13
 Madore, B. F., & Freedman, W. L. 1991, *PASP*, 103, 933
 Minniti, J. H., Sbordone, L., Rojas-Arriagada, A., et al. 2020, *A&A*, 640, A92
 Minniti, J. H., Zoccali, M., Rojas-Arriagada, A., et al. 2021, *A&A*, 654, A138
 O'Donnell, J. E. 1994, *ApJ*, 422, 158
 Pietrukowicz, P., Soszyński, I., & Udalski, A. 2021, *Acta Astron.*, 71, 205
 Planck Collaboration, Aghanim, N., Akrami, Y., et al. 2020, *A&A*, 641, A6
 Poggio, E., Drimmel, R., Cantat-Gaudin, T., et al. 2021, *A&A*, 651, A104
 Riess, A. G., Casertano, S., Yuan, W., Macri, L. M., & Scolnic, D. 2019, *ApJ*, 876, 85
 Riess, A. G., Casertano, S., Yuan, W., et al. 2021, *ApJ*, 908, L6
 Riess, A. G., Breuval, L., Yuan, W., et al. 2022b, *ApJ*, arXiv e-prints: arXiv:2208.01045
 Sana, H., Momany, Y., Gieles, M., et al. 2010, *A&A*, 515, A26
 Sim, G., Lee, S. H., Ann, H. B., & Kim, S. 2019, *J. Korean Astron. Soc.*, 52, 145
 Skinner, S. L., Zhekov, S. A., Palla, F., & Barbosa, C. L. D. R. 2005, *MNRAS*, 361, 191
 Soubiran, C., Cantat-Gaudin, T., Romero-Gómez, M., et al. 2018, *A&A*, 619, A155
 Turner, D. 1985, in *IAU Colloq. 82, Cepheids: Theory and Observation*, ed. B. F. Madore (New York: Cambridge Univ. Press), 209
 Turner, D. G. 1994, *J. Roy. Astron. Soc. Can.*, 88, 176
 Turner, D. G., & Burke, J. F. 2002, *AJ*, 124, 2931
 Turner, D. G., Abdel-Sabour Abdel-Latif, M., & Berdnikov, L. N. 2006, *PASP*, 118, 410
 Turner, D. G., Forbes, D., English, D., et al. 2008, *MNRAS*, 388, 444
 Turner, D. G. 2012a, *JAAVSO*, 40, 502
 Turner, D. G., Majaess, D. J., Lane, D. J., et al. 2012b, *MNRAS*, 422, 2501
 Zhou, X., & Chen, X. 2021, *MNRAS*, 504, 4768

Appendix A: Additional tables and figures

Table A.1. Parameters of the OC-Cepheid pairs identified in this work.

Cep name	Cep: α [deg]	Cep: δ [deg]	Cep: log(P) day	OC name	OC: α [deg]	OC: δ [deg]	Separation [arcmin]	OC: AD [arcmin]	Cep: μ_{α^*} [mas yr $^{-1}$]	Cep: μ_{δ} [mas yr $^{-1}$]	OC: μ_{α^*} [mas yr $^{-1}$]	OC: μ_{δ} [mas yr $^{-1}$]	Cep: π [mas]	OC: π [mas]	Cep: log(age) [yr]	OC: log(age) [yr]	OC: N	Num
CG Cas	0.25(0.01)	60.96(0.01)	0.64	Berkeley 58(*)	0.07(0.13)	60.94(0.06)	5.3	10.8	-3.24(0.01)	-1.67(0.01)	-3.48(0.09)	-1.81(0.09)	0.27(0.01)	0.29(0.02)	8.01(0.02)	7.78(0.16)	173	1
NO Cas	6.02(0.01)	61.34(0.01)	0.41	NGC 103(*)	6.31(0.12)	61.32(0.04)	8.4	8.4	-2.83(0.01)	-1.21(0.01)	-2.80(0.09)	-1.08(0.07)	0.27(0.01)	0.28(0.02)	8.04(0.06)	8.01(0.16)	173	2
DL Cas	7.49(0.02)	60.21(0.02)	0.90	NGC 129(*)	7.62(0.17)	60.20(0.07)	4.0	13.2	-2.71(0.03)	-1.19(0.03)	-2.59(0.12)	-1.19(0.11)	0.55(0.03)	0.53(0.03)	7.81(0.03)	8.11(0.16)	296	3
SU Cas	42.99(0.04)	68.89(0.04)	0.29	Alessi 95(*)	42.98(0.77)	68.89(0.21)	0.5	42.0	3.10(0.04)	-8.15(0.05)	1.46(0.34)	-7.94(0.41)	2.17(0.06)	2.28(0.06)	8.14(0.04)	8.20(0.10)	104	4
RS Ori	95.55(0.03)	14.68(0.02)	0.88	FSR 095(*)	95.58(0.09)	14.62(0.10)	3.5	16.8	0.20(0.04)	0.01(0.03)	0.22(0.10)	0.03(0.11)	0.56(0.03)	0.57(0.03)	7.83(0.02)	8.72(0.17)	146	5
CV Mon	99.27(0.01)	3.06(0.01)	0.73	vdBergh 1(*)	99.28(0.04)	3.08(0.03)	1.1	6.0	0.35(0.02)	-0.67(0.01)	0.40(0.13)	-0.71(0.12)	0.57(0.01)	0.55(0.04)	7.94(0.02)	7.61(0.15)	59	6
WX Pup	115.50(0.01)	25.88(0.01)	0.95	OC-0717(*)	115.29(0.24)	-26.03(0.28)	14.2	42.0	-2.97(0.01)	2.56(0.01)	-2.15(0.25)	2.25(0.43)	0.37(0.02)	0.37(0.01)	7.77(0.03)	8.28(0.17)	71	7
V335 Pup	119.24(0.01)	22.83(0.01)	0.69	UBC 229(*)	119.28(0.05)	-22.82(0.05)	2.0	12.0	-2.96(0.01)	2.89(0.02)	-2.98(0.06)	2.90(0.11)	0.42(0.02)	0.38(0.03)	7.81(0.11)	8.05(0.16)	57	8
J075840-3330.2	119.67(0.01)	-33.30(0.01)	0.64	UBC 1424(*)	119.70(0.09)	-33.58(0.07)	5.2	12.0	-2.34(0.01)	3.42(0.01)	-2.34(0.07)	3.27(0.16)	0.24(0.01)	0.24(0.01)	8.00(0.02)	7.66(0.15)	37	9
CS Vel	145.29(0.01)	-53.84(0.01)	0.77	Ruprecht 79(*)	145.26(0.06)	-53.84(0.04)	1.9	6.0	-4.57(0.01)	3.13(0.01)	-4.59(0.11)	3.02(0.09)	0.26(0.01)	0.24(0.02)	7.91(0.02)	7.79(0.16)	185	10
V Cen	218.14(0.01)	-56.89(0.01)	0.74	OC 5662(*)	218.77(0.37)	-56.67(0.21)	24.7	34.8	-6.70(0.02)	7.07(0.02)	-6.48(0.27)	-7.19(0.25)	1.39(0.02)	1.30(0.03)	7.93(0.02)	8.30(0.17)	244	11
V340 Nor	243.32(0.02)	-54.23(0.01)	1.05	NGC 6067(*)	243.31(0.08)	-54.23(0.05)	0.6	8.4	-2.07(0.03)	-2.63(0.02)	-1.97(0.14)	-2.58(0.14)	0.47(0.03)	0.47(0.03)	7.70(0.03)	8.10(0.16)	633	12
S Nor	244.72(0.02)	-57.90(0.01)	0.99	NGC 6687(*)	244.77(0.18)	-57.87(0.11)	2.2	16.8	-1.61(0.02)	-1.44(0.02)	-1.63(0.18)	-2.42(0.20)	1.08(0.02)	1.02(0.03)	7.74(0.03)	8.00(0.16)	157	13
OGLE-BLG-CEP-114(*)	260.81(0.04)	-44.33(0.03)	0.27	OC-0675(*)	260.78(0.06)	-44.39(0.04)	3.6	7.2	2.15(0.07)	-3.34(0.05)	2.12(0.17)	-3.26(0.15)	0.91(0.05)	0.88(0.03)	8.16(0.03)	7.70(0.18)	137	14
U Sgr	277.97(0.02)	-19.13(0.02)	0.83	IC-4725(*)	277.97(0.17)	-19.12(0.15)	0.4	26.4	-1.80(0.02)	-6.13(0.02)	-1.69(0.23)	-6.17(0.26)	1.57(0.02)	1.52(0.05)	7.87(0.02)	8.05(0.16)	399	15
V367 Sct	278.40(0.02)	-10.43(0.02)	0.80	NGC 6649(*)	278.36(0.05)	-10.40(0.05)	3.0	8.4	0.08(0.02)	-0.27(0.02)	0.03(0.15)	-0.12(0.15)	0.42(0.02)	0.47(0.05)	7.89(0.02)	7.85(0.16)	507	16
EV Sct	279.17(0.01)	-8.18(0.01)	0.49	NGC 6644(*)	279.13(0.06)	-8.18(0.05)	2.7	9.6	-0.21(0.02)	-2.55(0.01)	-0.07(0.14)	-2.59(0.13)	0.49(0.02)	0.46(0.04)	7.97(0.07)	8.35(0.17)	214	17
GQ Vul	296.99(0.01)	26.00(0.02)	1.10	FSR 0158(*)	297.00(0.05)	26.04(0.05)	2.2	8.4	-2.81(0.02)	-5.47(0.02)	-2.77(0.08)	-5.50(0.10)	0.14(0.02)	0.14(0.01)	7.66(0.03)	7.81(0.25)	145	18
X Vul	299.37(0.01)	26.56(0.02)	0.80	UBC 129(*)	299.09(0.16)	26.48(0.16)	3.7	26.4	-1.35(0.02)	-4.25(0.02)	-1.00(0.15)	-4.35(0.20)	0.84(0.02)	0.85(0.02)	7.72(0.15)	8.35(0.15)	145	19
G1 Cyg	299.89(0.01)	33.75(0.01)	0.76	UBC 135(*)	299.82(0.06)	33.73(0.04)	15.6	7.2	-3.45(0.01)	-6.58(0.02)	-3.52(0.08)	-6.45(0.10)	0.25(0.01)	0.24(0.03)	7.92(0.02)	7.38(0.15)	88	20
J20151.18+342447.2	302.96(0.01)	34.41(0.01)	0.99	Berkeley 51(*)	303.01(0.05)	34.39(0.05)	2.6	7.2	-3.18(0.01)	-4.91(0.02)	-3.06(0.10)	-4.84(0.12)	0.19(0.01)	0.15(0.02)	7.74(0.03)	7.98(0.16)	64	21
V1788 Cyg	310.65(0.02)	38.46(0.02)	1.15	OC-0125(*)	310.77(0.09)	38.45(0.05)	5.3	10.8	-0.91(0.02)	-4.45(0.02)	-2.74(0.17)	-4.28(0.17)	0.35(0.02)	0.34(0.03)	7.63(0.03)	7.50(0.17)	74	22
J2116594+514556.7	319.25(0.02)	51.77(0.01)	0.77	Berkeley 55(*)	319.24(0.06)	51.77(0.03)	0.5	6.0	-3.91(0.02)	-4.72(0.02)	-4.70(0.15)	-4.65(0.14)	0.32(0.02)	0.32(0.05)	7.91(0.02)	8.30(0.17)	104	23
J213533.70+533049.3	323.89(0.01)	53.51(0.01)	0.51	Kronberger 84(*)	323.91(0.18)	53.53(0.11)	1.2	18.0	-2.88(0.01)	-3.11(0.01)	-2.92(0.17)	-3.03(0.15)	0.19(0.01)	0.19(0.03)	7.96(0.08)	8.46(0.17)	93	24
CE Cas B	359.54(0.01)	61.21(0.01)	0.65	NGC 7790(*)	359.61(0.08)	61.21(0.03)	2.1	6.0	-3.30(0.01)	-1.81(0.02)	-3.23(0.09)	-1.73(0.08)	0.31(0.02)	0.29(0.03)	8.00(0.02)	8.11(0.16)	159	25
CH Cas A	359.54(0.01)	61.21(0.01)	0.71	NGC 7790(*)	359.61(0.08)	61.21(0.03)	2.1	6.0	-3.30(0.01)	-1.81(0.02)	-3.23(0.09)	-1.73(0.08)	0.31(0.02)	0.29(0.03)	8.00(0.02)	8.11(0.16)	159	25
CF Cas	359.57(0.01)	61.22(0.01)	0.69	NGC 7790(*)	359.61(0.08)	61.21(0.03)	1.3	6.0	-3.24(0.01)	-1.77(0.01)	-3.23(0.09)	-1.73(0.08)	0.29(0.01)	0.29(0.03)	7.97(0.02)	8.11(0.16)	159	25

Notes. Class A: Cepheids are related to OCs and have been identified as cluster members.; Class C: Cepheids may be unrelated to OCs but they possess similar astrometric parameters. The astrometric parameters for each classical Cepheid (Cep) are from *Gaia* DR3. Separation is the angular distance between a Cepheid and its host OC. For each OC, its astrometric parameters, corresponding standard deviations, and apparent angular diameter (AD) are derived from the literature, and those of newly found OCs were estimated in this work. Asterisks associated with Cepheid names indicate that these Cepheid may not fall within the instability strip. OC names with asterisks show that they have some *Gaia* RV measurements. The table can be found at the CDS.

Table A.2. Parameters of the proposed newly found OCs ordered by increasing l .

ID	α [deg]	δ [deg]	l [deg]	b [deg]	θ [deg]	ϖ [mas]	μ_{α^*} [mas yr ⁻¹]	μ_{δ} [mas yr ⁻¹]	log(age) [yr]	A_G [mag]	DM [mag]	V_r [km s ⁻¹]	N (N_r)
OC-0705(*)	268.56(0.11)	-23.14(0.09)	5.97(0.09)	1.31(0.09)	0.13	0.74(0.01)	0.10(0.23)	-2.64(0.25)	7.50(0.17)	2.48	10.86	-5.40(-)	30(1)
OC-0706(*)	278.38(0.04)	-10.40(0.04)	21.65(0.04)	-0.80(0.04)	0.06	0.54(0.01)	-0.01(0.17)	-0.12(0.17)	8.46(0.19)	4.04	10.95	-18.24(-)	26(1)
OC-0707(*)	278.37(0.06)	-10.39(0.06)	21.65(0.06)	-0.79(0.06)	0.09	0.40(0.01)	0.03(0.17)	-0.14(0.16)	7.72(0.18)	4.04	11.19	-9.37(-)	58(1)
OC-0708	282.68(0.05)	-6.35(0.05)	27.19(0.05)	-2.73(0.05)	0.07	0.37(0.01)	-1.56(0.13)	-4.23(0.13)	6.92(0.16)	2.26	12.53	-(-)	39(0)
OC-0709(*)	290.72(0.15)	18.67(0.14)	53.06(0.16)	1.75(0.12)	0.20	0.95(0.02)	-1.01(0.27)	-6.14(0.27)	7.88(0.18)	2.62	9.90	-10.80(15.39)	47(5)
OC-0710(*)	292.64(0.04)	20.26(0.05)	55.32(0.06)	0.92(0.03)	0.06	0.28(0.01)	-2.81(0.08)	-6.44(0.11)	8.32(0.19)	3.66	12.20	24.56(22.24)	32(4)
OC-0711(*)	295.73(0.18)	20.03(0.18)	56.54(0.18)	-1.72(0.18)	0.25	1.09(0.05)	-0.50(0.40)	-5.45(0.43)	7.74(0.18)	1.78	9.41	-18.07(34.56)	55(11)
OC-0712(*)	304.72(0.06)	37.75(0.06)	75.72(0.07)	0.98(0.04)	0.08	0.30(0.01)	-2.95(0.13)	-4.67(0.09)	8.00(0.18)	3.76	12.65	-35.07(-)	34(1)
OC-0713(*)	351.27(0.33)	61.32(0.10)	112.76(0.17)	0.16(0.08)	0.19	0.30(0.01)	-3.94(0.15)	-2.17(0.11)	7.00(0.16)	2.68	12.60	63.16(8.10)	26(2)
OC-0714	26.04(0.13)	61.88(0.05)	129.10(0.06)	-0.36(0.05)	0.08	0.38(0.01)	-1.12(0.12)	-0.31(0.11)	7.22(0.17)	2.70	11.89	-(-)	51(0)
OC-0715(*)	59.94(0.40)	55.54(0.27)	147.43(0.30)	1.90(0.18)	0.35	0.22(0.02)	-0.01(0.11)	-0.05(0.11)	6.80(0.14)	3.08	13.05	-38.52(10.95)	307(3)
OC-0716(*)	99.64(0.12)	2.08(0.10)	209.61(0.12)	-1.91(0.11)	0.16	0.51(0.01)	-1.09(0.15)	-2.02(0.13)	9.32(0.21)	1.24	11.26	35.10(6.27)	63(4)
OC-0717(*)	115.29(0.24)	-26.03(0.28)	241.55(0.29)	-1.60(0.21)	0.35	0.37(0.01)	-2.15(0.25)	2.25(0.43)	8.28(0.17)	1.14	11.95	55.82(31.47)	71(4)
OC-0718(*)	110.65(0.21)	-29.86(0.14)	242.96(0.13)	-7.03(0.20)	0.23	0.12(0.01)	-0.73(0.11)	1.87(0.21)	8.65(0.17)	0.38	14.70	91.92(121.58)	45(3)
OC-0719(*)	123.11(0.09)	-27.93(0.07)	246.80(0.07)	3.35(0.08)	0.11	0.37(0.01)	-1.60(0.06)	2.90(0.09)	9.20(0.21)	0.54	11.94	27.71(8.29)	71(8)
OC-0720(*)	122.19(0.11)	-36.16(0.17)	253.27(0.18)	-1.79(0.06)	0.19	2.78(0.06)	-7.51(0.20)	11.41(0.51)	6.32(0.13)	2.40	7.58	30.73(31.17)	15(5)
OC-0721(*)	127.19(0.10)	-41.19(0.14)	259.62(0.13)	-1.40(0.09)	0.16	0.25(0.01)	-2.92(0.12)	3.49(0.28)	7.58(0.15)	3.16	12.82	73.17(-)	22(1)
OC-0722(*)	130.66(0.06)	-47.20(0.05)	265.93(0.04)	-3.02(0.04)	0.06	0.41(0.01)	-2.72(0.12)	5.22(0.13)	8.46(0.19)	1.52	11.96	19.07(-)	41(1)
OC-0723(*)	132.34(0.11)	-46.56(0.11)	266.15(0.11)	-1.72(0.08)	0.14	0.19(0.02)	-3.25(0.15)	3.61(0.17)	7.46(0.15)	2.32	13.40	96.90(4.86)	116(2)
OC-0724	137.95(0.10)	-52.23(0.04)	272.82(0.05)	-2.70(0.05)	0.07	0.33(0.01)	-4.06(0.06)	3.95(0.05)	8.38(0.19)	1.48	12.20	-(-)	27(0)
OC-0725(*)	139.16(0.09)	-54.16(0.04)	274.71(0.05)	-3.50(0.05)	0.07	0.20(0.01)	-3.58(0.05)	2.72(0.09)	8.86(0.20)	1.22	13.30	17.18(9.11)	37(10)
OC-0726(*)	149.41(0.11)	-54.60(0.06)	279.46(0.07)	0.15(0.06)	0.09	0.23(0.01)	-5.01(0.07)	4.48(0.07)	8.98(0.21)	1.46	12.97	29.67(6.21)	47(7)
OC-0727	159.27(0.13)	-59.92(0.05)	286.83(0.06)	-1.32(0.06)	0.08	0.26(0.01)	-5.70(0.11)	2.48(0.11)	7.00(0.16)	2.08	12.94	-(-)	33(0)
OC-0728(*)	161.18(0.05)	-59.35(0.03)	287.40(0.03)	-0.35(0.03)	0.04	0.38(0.01)	-6.13(0.14)	2.10(0.12)	6.74(0.16)	1.74	12.12	-26.28(-)	33(1)
OC-0729(*)	160.61(0.15)	-60.43(0.09)	287.66(0.08)	-1.44(0.08)	0.11	0.24(0.01)	-5.58(0.11)	2.61(0.08)	8.76(0.20)	1.20	13.48	22.35(-)	32(1)
OC-0730(*)	168.63(0.10)	-57.56(0.04)	290.20(0.06)	2.90(0.04)	0.07	0.46(0.01)	-1.65(0.09)	-1.22(0.09)	9.44(0.22)	0.62	11.90	-24.12(13.14)	30(2)
OC-0731(*)	172.62(0.07)	-60.76(0.03)	293.20(0.03)	0.58(0.03)	0.04	0.22(0.01)	-6.86(0.08)	1.37(0.08)	8.96(0.21)	1.52	12.71	3.17(3.27)	31(6)
OC-0732(*)	181.53(0.09)	-62.62(0.03)	297.75(0.04)	-0.21(0.03)	0.05	0.28(0.01)	-8.28(0.10)	0.95(0.06)	8.66(0.20)	1.56	12.53	-2.87(53.36)	28(2)
OC-0733	193.44(0.14)	-60.36(0.07)	303.22(0.07)	2.51(0.07)	0.10	0.54(0.01)	-4.65(0.20)	-1.07(0.16)	7.42(0.17)	1.08	11.15	-(-)	37(0)
OC-0734	194.51(0.08)	-64.96(0.03)	303.63(0.04)	-2.10(0.03)	0.05	0.24(0.01)	-5.84(0.11)	-0.94(0.09)	8.48(0.20)	2.52	12.48	-(-)	26(0)
OC-0735(*)	223.62(0.20)	-57.63(0.09)	318.83(0.11)	1.40(0.08)	0.14	0.89(0.02)	-3.34(0.14)	-2.62(0.15)	7.86(0.18)	2.08	10.46	-31.08(5.21)	26(3)
OC-0736(*)	230.27(0.11)	-59.60(0.06)	320.85(0.07)	-2.04(0.05)	0.08	0.30(0.01)	-3.94(0.13)	-3.55(0.12)	6.70(0.15)	3.94	13.02	-8.85(137.18)	30(2)
OC-0737(*)	240.21(0.09)	-53.54(0.06)	328.85(0.06)	-0.48(0.06)	0.08	0.41(0.01)	-4.24(0.14)	-4.78(0.13)	8.82(0.20)	2.40	11.73	-30.69(35.72)	92(3)
OC-0738(*)	242.58(0.09)	-52.33(0.06)	330.72(0.06)	-0.53(0.05)	0.08	0.35(0.01)	-2.93(0.11)	-4.27(0.10)	8.42(0.19)	3.42	11.66	-18.24(7.77)	38(6)
OC-0739(*)	252.33(0.07)	-44.73(0.06)	340.66(0.06)	0.02(0.05)	0.08	0.41(0.01)	-1.32(0.12)	-2.54(0.11)	7.72(0.18)	2.70	11.33	-38.73(-)	67(1)
OC-0740(*)	252.32(0.07)	-44.71(0.05)	340.68(0.05)	0.04(0.06)	0.07	0.39(0.01)	-1.33(0.09)	-2.54(0.11)	8.00(0.18)	2.64	11.47	-72.58(48.38)	32(2)
OC-0741(*)	264.91(0.07)	-33.21(0.06)	355.70(0.06)	-1.16(0.06)	0.08	0.38(0.01)	0.12(0.15)	-0.76(0.12)	6.98(0.16)	4.04	11.49	111.11(160.56)	61(6)
OC-0742	262.93(0.09)	-31.97(0.09)	355.84(0.08)	0.91(0.09)	0.12	0.35(0.01)	-0.82(0.23)	-1.81(0.22)	8.00(0.18)	4.04	12.26	-(-)	27(0)

Notes. The listed parameters of each OC are mean astrometric parameters, corresponding standard deviations, and the apparent angular radius (θ), all of which are from the member stars (N) and stars with RV measurements (N_r). Ages (log(age)), line-of-sight extinction (A_G), and DM are also provided. OC names marked with an asterisk have a *Gaia* RV measurement. The table is available at the CDS.

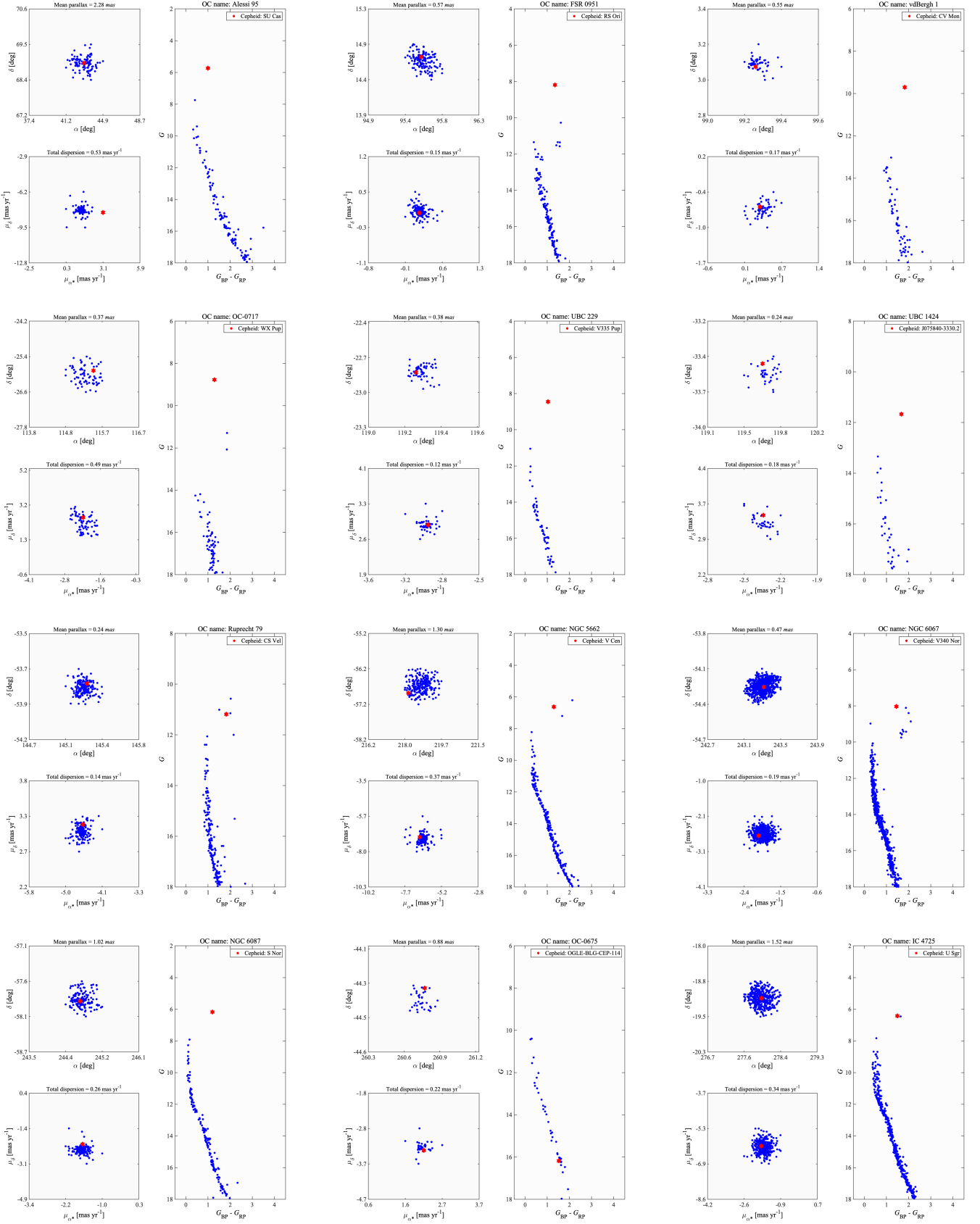


Fig. A.1. Open clusters (blue dots) harboring classical Cepheids (red hexagram). The columns of each panel represent the distributions of the member stars of OCs and classical Cepheids for position in RA (α) and Dec (δ), proper motions in μ_{α^*} and μ_{δ} , and the CMD in G vs. $G_{BP} - G_{RP}$, as well as the mean parallax and total proper-motion dispersion of OCs. Here, the listed OCs are Alessi 95, FSR 0951, vdBergh 1, OC-0717, UBC 229, UBC 1424, Ruprecht 79, NGC 5662, NGC 6067, NGC 6087, OC-0675, and IC 4725.

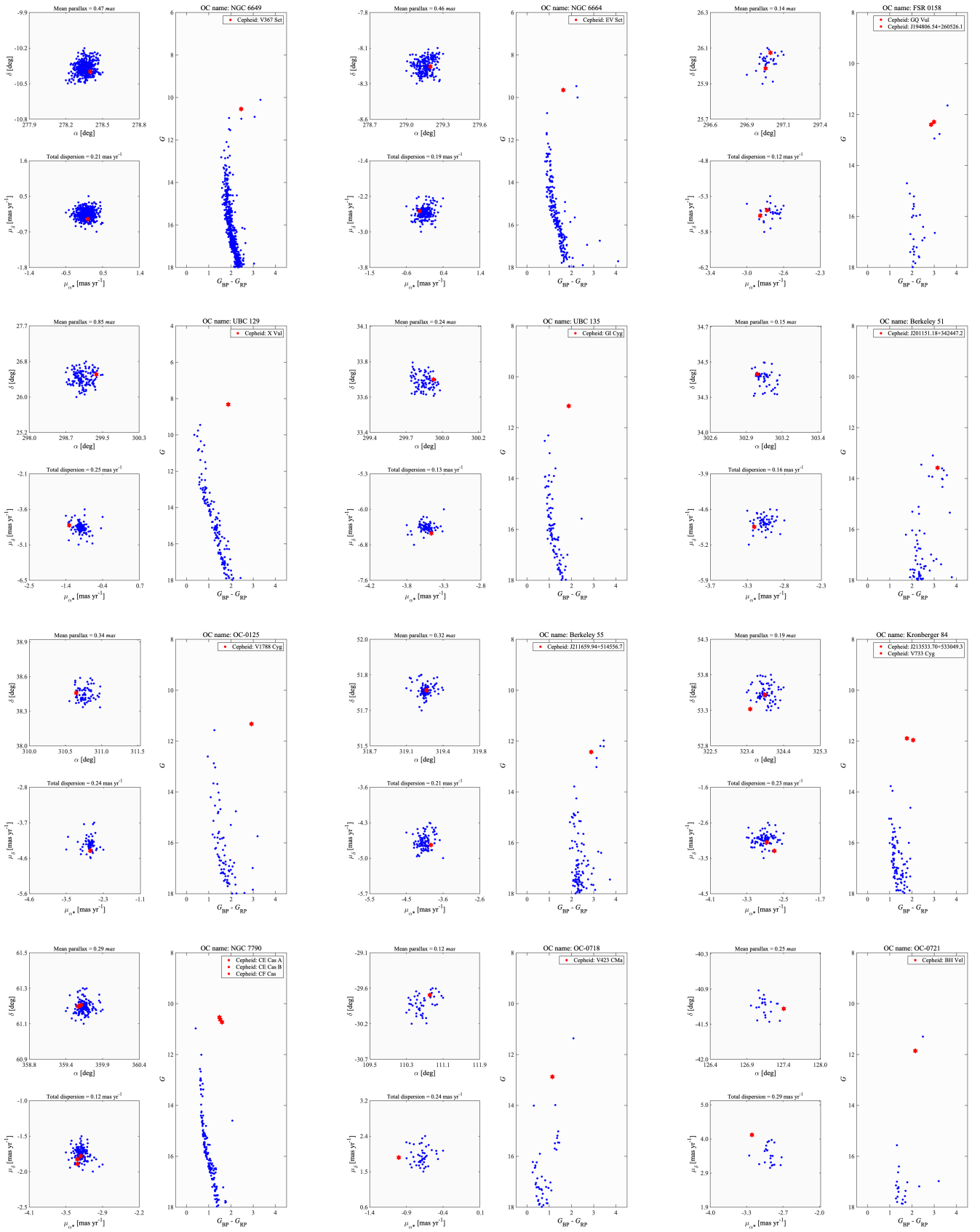


Fig. A.1. continued. Here, the listed OCs are NGC 6649, NGC 6664, FSR 0158, UBC 129, UBC 135, Berkeley 51, OC-0125, Berkeley 55, Kronberger 84, NGC 7790, OC-0718, and OC-0721.

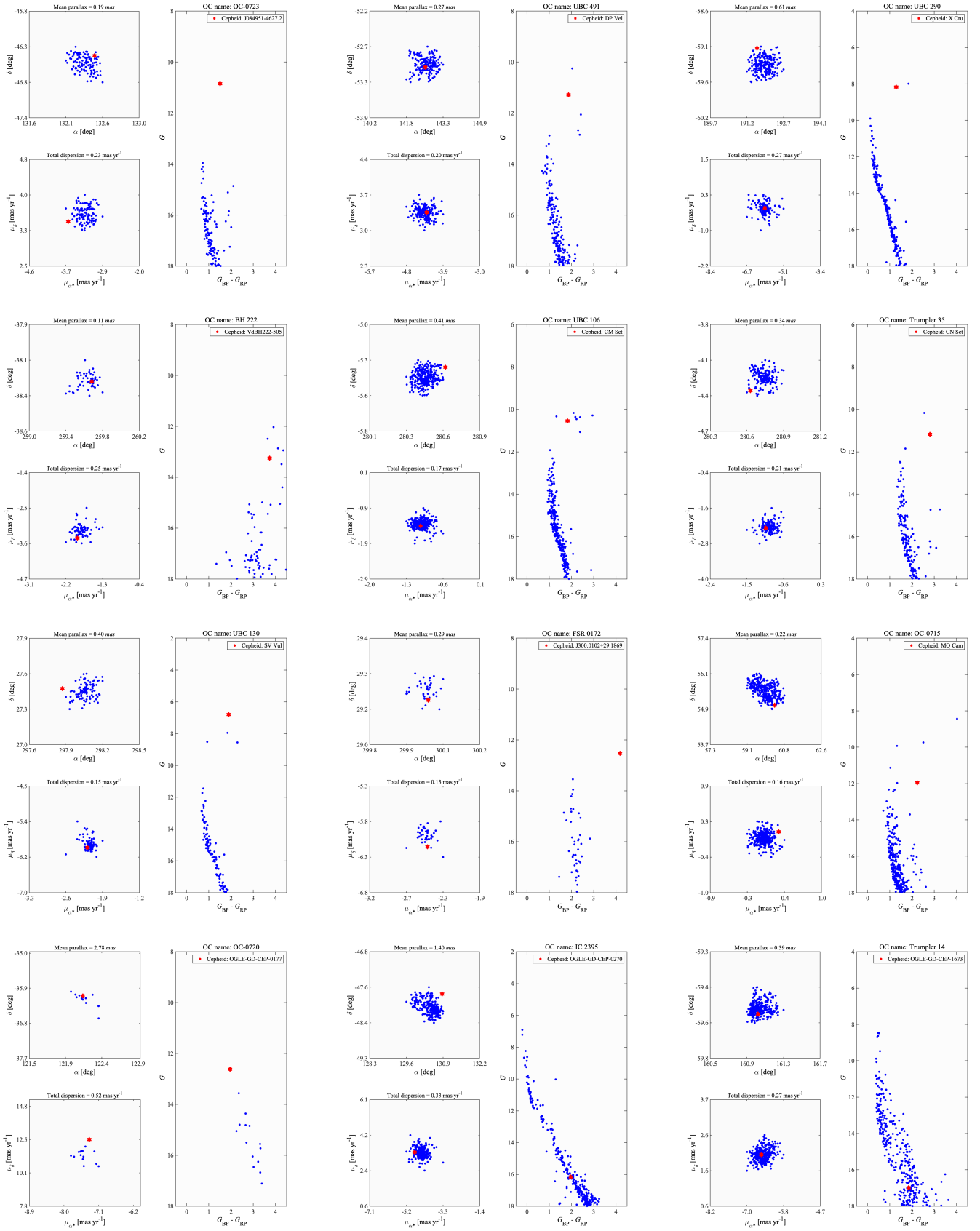


Fig. A.1. continued. Here, the listed OCs are OC-0723, UBC 491, UBC 290, BH 222, UBC 106, Trumpler 35, UBC 130, FSR 0172, OC-0715, OC-0720, IC 2395, and Trumpler 14.

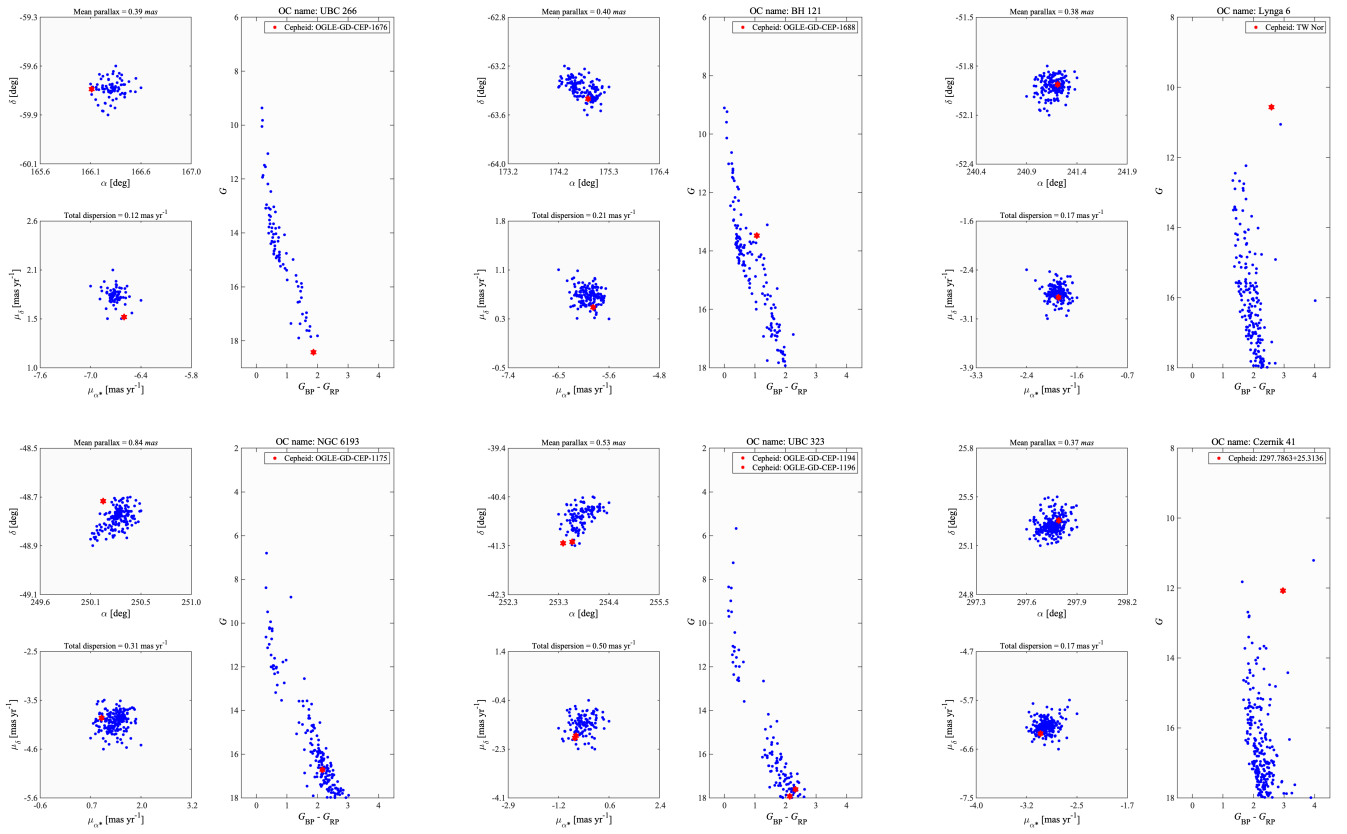


Fig. A.1. continued. Here, the listed OCs are UBC 266, BH 121, Lynga 6, NGC 6193, UBC 323, and Czernik 41.